Proc. Natl. Acad. Sci. USA
Vol. 93, pp. 2493–2498, March 1996
Biochemistry

Visualization of intermediate and transition-state structures in protein-tyrosine phosphatase catalysis

JOHN M. DENU*, DANIEL L. LOHSE*, J. VIJAYALAKSHMI†, MARK A. SAPER*†, AND JACK E. DIXON*‡

*Department of Biological Chemistry, †Biophysics Research Division and the Walther Cancer Institute, University of Michigan, Ann Arbor, MI 48109-0606

Communicated by J. L. Oncley, University of Michigan, Ann Arbor, MI, November 20, 1995 (received for review August 29, 1995)

ABSTRACT **Engineering site-specific amino acid substitutions into the protein-tyrosine phosphatase (PTPase) PTP1 and the dual-specific vaccinia H1-related phosphatase (VHR), has kinetically isolated the two chemical steps of the reaction and provided a rare opportunity for examining transition states and directly observing the phosphoenzyme intermediate. Changing serine to alanine in the active-site sequence motif HCXXGXXRS shifted the rate-limiting step from intermediate formation to intermediate hydrolysis. Using phosphorus ^{31}P NMR, the covalent thiol–phosphate intermediate was directly observed during catalytic turnover. The importance of the conserved aspartic acid (D92 in VHR and D181 in PTP1) in both chemical steps was established. Kinetic analysis of D92N and D181N mutants indicated that aspartic acid acts as a general acid by protonating the leaving-group phenolic oxygen. Structure–reactivity experiments with native and aspartate mutant enzymes established that proton transfer is concomitant with P–O cleavage, such that no charge develops on the phenolic oxygen. Steady- and presteady-state kinetics, as well as NMR analysis of the double mutant D92N/S131A (VHR), suggested that the conserved aspartic acid functions as a general base during intermediate hydrolysis. As a general base, aspartate would activate a water molecule to facilitate nucleophilic attack. The amino acids involved in transition-state stabilization for cysteinylphosphate hydrolysis were confirmed by the x-ray structure of the *Yersinia* PTPase complexed with vanadate, a transition-state mimic that binds covalently to the active-site cysteine. Consistent with the NMR, x-ray, biochemical, and kinetic data, a unifying mechanism for catalysis is proposed.**

Protein-tyrosine phosphatases (PTPases) are a large family of enzymes that catalyze the hydrolysis of phosphotyrosine from specific proteins. The importance of these catalysts in signal-transduction pathways is evident from their roles in T-cell activation (1), antigen-receptor signaling in B cells (2), and the function of the PTPase FAP-1 in inhibiting FAS receptor-activated programmed cell death (3). *Yersinia*, the genus of bacteria responsible for the bubonic plague, has been shown to harbor the most reactive PTPase described to date, and the corresponding PTPase gene has been shown to be a virulence determinant in this disease process (4, 5).

The first phosphatase capable of dephosphorylating proteins containing phospho-Ser/Thr and -Tyr was shown to be encoded by an open reading frame in the vaccinia virus (6). This family of phosphatases includes a human phosphatase related to the vaccinia phosphatase [vaccinia H1-related phosphatase (VHR)] (7), the cell-cycle phosphatase (8, 9) $p80^{cdc25}$, and mitogen-activated protein (MAP) kinase phosphatases (10, 11). They are now commonly referred to as dual-specific phosphatases.

Although the biological roles of the PTPases and the dual-specific phosphatases are distinct, recent evidence suggests that both classes of enzymes employ a similar mechanism to hydrolyze phosphate monoesters. A common mechanism is strongly substantiated by the current study. These catalysts share the active-site sequence motif HCXXGXXRS(T). The cysteine is required for catalysis and appears to be the nucleophile that forms a thiol–phosphate intermediate during catalysis (12–14). The crystal structures of PTP1B and the *Yersinia* PTPase revealed a conserved active-site loop where the cysteine rests at the base of the active-site cleft, consistent with an in-line nucleophilic attack of the thiolate on the phosphorus monoester center (15, 16). The involvement of an aspartic acid as a general acid has been demonstrated for VHR (17) and the *Yersinia* PTPase (18). The minimal kinetic mechanism of these phosphatases can be defined by two chemical steps (Scheme I) and two transition states. Formation and hydrolysis of the intermediate are denoted by k_3 and k_5, respectively.

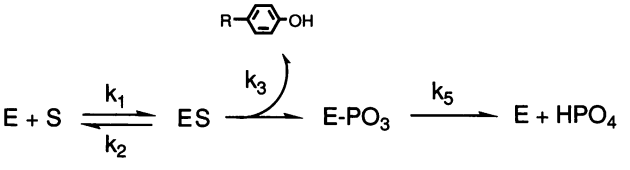

Scheme I

In the current study, we have engineered site-specific amino acid substitutions in PTP1 and the dual-specific phosphatase VHR, which have kinetically isolated the two chemical steps in the reaction (i.e., k_3 and k_5), providing a rare opportunity for examining transition states and for directly observing the intermediate during catalysis.

MATERIALS AND METHODS

Materials. All chemicals were of the highest purity commercially available. Enzymes were overexpressed in *E. coli* using a T7 polymerase-base expression system and were purified to homogeneity as judged by SDS/PAGE. Purification of all VHR enzymes was done as described (19). The rat homolog, PTP1, of human PTP1B was used in these studies (12). The PTP1 enzymes are truncated at residue 323 of the C terminus and were purified using phenyl-Sepharose and S-Sepharose column chromatography. The native and mutant enzymes have identical chromatographic properties and have identical CD spectra, strongly suggesting the absence of any significant structural changes induced by the conservative substitutions.

Mutagenesis. Site-directed mutagenesis of PTP1 was done as described (17). Verification was provided by DNA sequencing. D92N/S131A VHR was constructed from preexisting pT7-VHR expression vectors containing the single amino acid

The publication costs of this article were defrayed in part by page charge payment. This article must therefore be hereby marked "*advertisement*" in accordance with 18 U.S.C. §1734 solely to indicate this fact.

Abbreviations: PTPase, protein-tyrosine phosphatase; VHR, vaccinia H1-related phosphatase; *p*NPP, *p*-nitrophenylphosphate.

‡To whom reprint requests should be addressed.

Table 1. Effects of amino acid substitutions at conserved aspartic acid and serine residues in the protein-tyrosine phosphatase PTP1 and the dual-specific phosphatase VHR

Enzyme	k_{cat}, s^{-1}	k_{cat}/K_m, $s^{-1}\cdot M^{-1}$	K_i, mM	k_3, s^{-1}
VHR	5.5	3.2×10^3	0.97	
S131A VHR	6.0×10^{-2}	1.0×10^3	0.65	7.0 (pH 6) 1.2 (pH 8)
D92N VHR	6.0×10^{-2}	1.4×10^2		
S131A/D92N VHR	9.0×10^{-4}	1.1×10^2		9.7×10^{-2} (pH 6) 6.0×10^{-1} (pH 9)
PTP1	20	4.6×10^4	1.4	
S222A PTP1	2.0×10^{-1}	5.2×10^3	2.8	15
D181N PTP1	4.2×10^{-1}	8.3×10^2		

All assays were performed and analyzed as described in text and in ref. 20. Standard errors were routinely 5% and not >20% for any individual rate.

change and taking advantage of a unique *Pfl*m restriction site located between the two mutations. An insert (*Pfl*m1 and *Eco*RI) containing the S131A mutation was ligated into the pT7-(VHR-D92N) vector digested with *Pfl*m and *Eco*RI. The double mutation D92N/S131A was confirmed by DNA sequencing.

Steady-State and Rapid-Reaction Kinetic Analysis. The steady-state and rapid-reaction kinetic analysis was done as described (20). Enzyme and pNPP (*p*-nitrophenyl phosphate) were rapidly mixed using a stopped-flow spectrophotometer (Applied Photophysics, Leatherhead, U.K.) and the product pNP (*p*-nitrophenol) was followed at 405 nm. When 4-methylumbelliferyl phosphate was used as substrate, the product was followed at 370 nm. The enzyme concentration ranged from 25 to 100 μM, and substrate concentrations were kept high enough (2–10 mM) to saturate the enzymes. The pH-dependence of the kinetics was accomplished in 0.1 M acetate/0.05 M Tris/0.05 M Bis-Tris (30°C), a buffer that maintains constant ionic strength over a wide pH range. Because of the slower burst rate for the D92N/S131A enzyme, kinetic traces were collected on both stopped-flow and standard spectrophotometers (Perkin Elmer Lambda 6).

Phosphorus NMR. D92N/S131A VHR (1.1 mM) and 3.0 mM *p*NPP were mixed in a 5-mm NMR tube at 22°C containing 0.1 M acetate, 0.05 M Tris, and 0.05 M Bis-Tris, pH 7.0. NMR spectra were obtained with a General Electric GNΩ500 at 202.477 MHz in ^3H_2O. Chemical shifts are reported in ppm relative to 80% H_3PO_4. The spectra were obtained with 0.25sec delay between pulses. The 0-min, 13-min, 19-min, 28-min, 40-min, and 2-day spectra were acquired in 400, 300, 500, 800, 1200, and 850 scans, respectively. The chemical shifts were assigned by obtaining spectra for each separately. The thiol–phosphate chemical shift is consistent with previous assignments (13).

Leaving Group Dependence. Substrates *p*NPP (pK_a = 7.1), 4-methylumbelliferyl phosphate (7.8), β-naphthyl phosphate (9.38), phenyl phosphate (9.99), and phosphotyrosine (10.07) in the peptide DHTGFLTEYVATR corresponding to mitogen-activated protein (MAP) kinase were used in the study of native VHR and PTP1 and their corresponding mutants, D92N and D181N. The assay conditions were 0.1 M acetate, 0.05 M Tris and 0.05 M Bis-Tris, pH 7.0 and 30°C. The k_{cat} and k_{cat}/K_m values were calculated by using previously determined extinction coefficients (21). With 4-methylumbelliferyl phosphate, an $\Sigma_{370nm} = 2.22\ mM^{-1}\cdot cm^{-1}$ at pH 7.0 was calculated and used in both the steady-state and rapid reaction analysis.

RESULTS AND DISCUSSION

Loss of Conserved Hydroxyl Residue Alters the Rate-Limiting Step. We demonstrate that changing serine to alanine in the active-site sequence motif HCXXGXXRS shifted the rate-limiting step from intermediate formation to intermediate hydrolysis. The loss of this conserved hydroxyl residue in both VHR (S131A) (20) and PTP1 (S222A) greatly diminishes the ability of these enzymes to catalyze phosphoenzyme hydrolysis without significantly affecting binding and intermediate formation. Between pH 4.5 and 9.0, the S131A VHR and S222A PTP1 enzymes exhibited a 2- to 20-fold decrease in k_{cat}/K_m values (k_1k_3/k_2+k_3), whereas the values for k_{cat} (k_3k_5/k_3+k_5) exhibited a dramatic 100-fold decrease. Results at pH 6 are listed in Table 1. The k_{cat}/K_m pH profile was identical between native and Ser → Ala enzymes. Moreover, the inhibition constant for the competitive inhibitor phosphate (K_i = 1.43 mM) is not significantly different than that obtained for native PTP1 (K_i = 2.77 mM). The change in rate-limiting step was confirmed using rapid-reaction kinetics. The kinetic traces of the S131A VHR and S222A PTP1 enzymes displayed a rapid exponential burst of product (*p*NP) followed by a slower linear rate. The rate of burst corresponds to intermediate formation (k_3), and the slow linear rate represents ($k_5 = k_{cat}$) intermediate hydrolysis. The amplitude of the burst was stoichiometric with final enzyme concentration. Because intermediate formation is rate-limiting with the native enzymes, no pre-steady-state burst was detected under the identical conditions. From the rapid kinetics, the PTP1 S222A mutant has a k_3 (rate of intermediate formation) value of 15 s^{-1} which agrees well with the k_{cat} value of 20 s^{-1} observed for the native enzyme (Table 1). Rapid-reaction kinetic analysis of S222A PTP1 and S131A VHR suggested that the phosphoenzyme intermediate was present at stoichiometric amounts, following the initial burst of product formation.

The crystal structures of PTP1B and the *Yersinia* PTPase indicated that the conserved hydroxyl residue was within hydrogen bonding distance (≈3 Å) to the cysteine nucleophile (16, 22). Although hydrogen bonds with cysteine are not a common feature of globular proteins (23), there is evidence for hydrogen bonding to cysteine in proteins (23, 24) and other sulfur-containing model compounds (25). A recent NMR report (26) on thioredoxin has strongly suggested that a proton is shared between the catalytic thiolate anion (Cys-32) and the adjacent thiol (Cys-35). A hydrogen bond to cysteine in the phosphatases could assist in stabilizing the developing negative charge during intermediate hydrolysis, making the thiolate a better leaving group (Scheme II). Alternatively, the hydroxyl could assist in positioning the thiol–phosphate for efficient in-line attack by the nucleophilic water molecule.

Conserved Aspartic Acid Functions as a General Acid During Intermediate Hydrolysis. To further explore the transition state for intermediate hydrolysis, we tested the possibility that the conserved aspartate residue might function as a general base during intermediate hydrolysis (Scheme II).

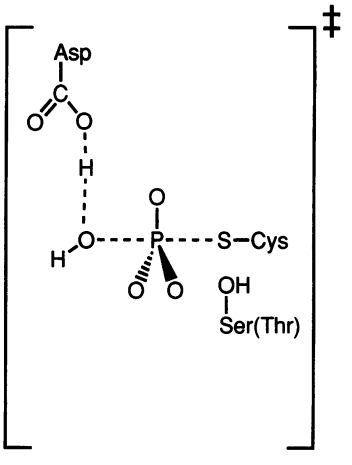

Scheme II

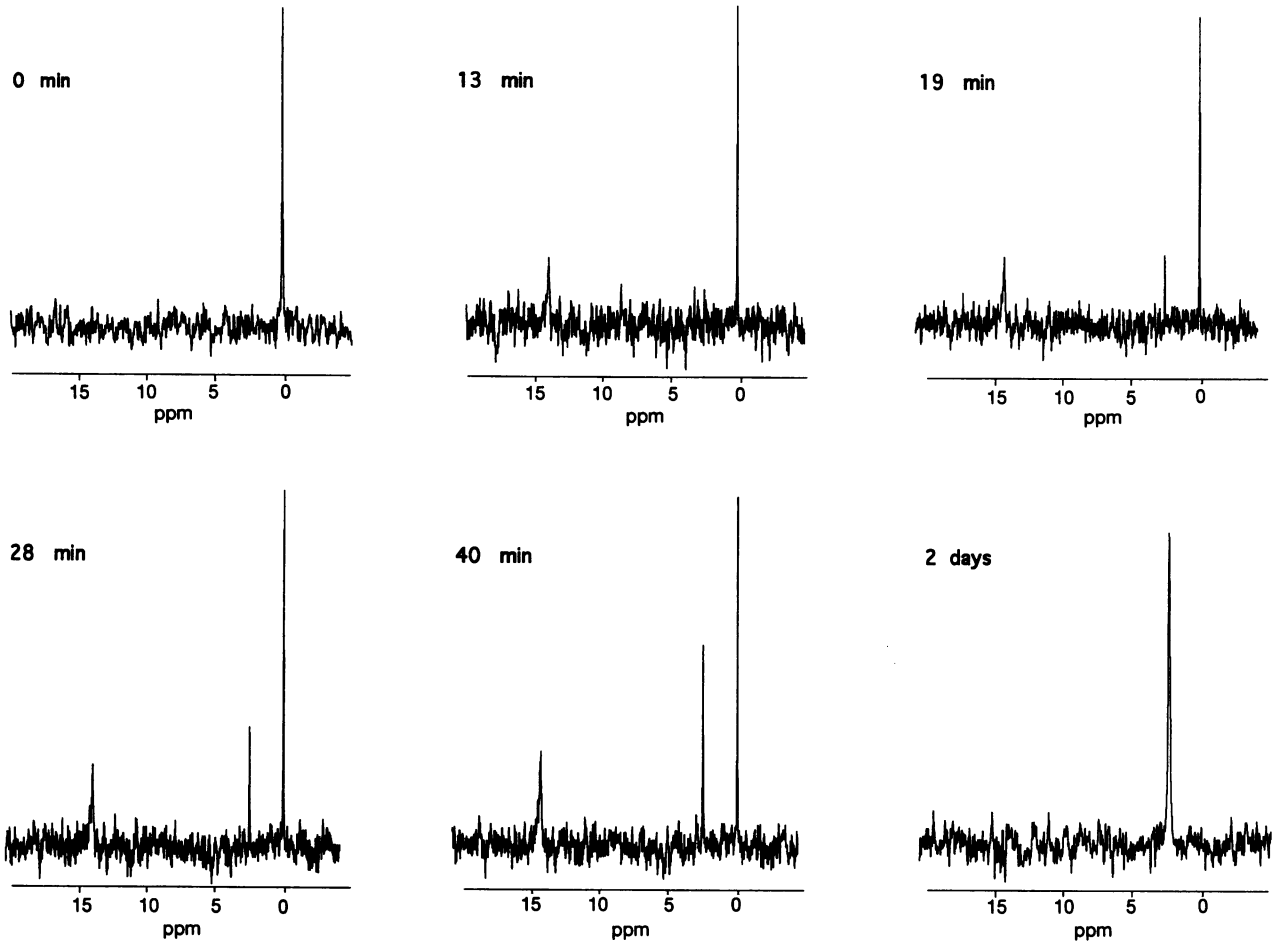

FIG. 1. ^{31}P NMR of the cysteinylphosphate intermediate of the dual-specific phosphatase VHR during catalytic turnover. Three resonances were observed. The resonance at 0.1 ppm corresponds to *p*NPP, the resonance at 2.4 ppm corresponds to free phosphate, and the resonance at 13.7 corresponds to the thiol–phosphate intermediate. The chemical shifts were assigned by obtaining spectra for each separately. The thiol–phosphate chemical shift is consistent with previous assignments (13). D92N/S131A VHR (1.1 mM) and 3.0 mM pNPP were mixed in a 5 mm NMR tube at 22°C in 0.1 M acetate/0.05 M Tris/0.05 M Bis-Tris, pH 7.0. NMR spectra were obtained with a General Electric model GNΩ500 instrument at 202.477 MHz in ^3H_2O. Chemical shifts are reported in ppm relative to 80% H_3PO_4.

Hydrolysis of the thiol–phosphate intermediate is expected to be facilitated by general base catalysis, which would activate a water molecule by proton abstraction. Therefore, mutations at the conserved aspartate residue would also slow the rate of intermediate hydrolysis. Because intermediate formation is rate-limiting with the native enzymes, it was impossible to probe the role of the aspartate residue as a general base during intermediate hydrolysis. This problem was solved by engineering VHR to contain both the D92N and S131A substitutions. The S131A substitution offers an opportunity to kinetically isolate intermediate hydrolysis because it does not significantly affect binding or intermediate formation but slows intermediate hydrolysis such that it becomes rate-limiting. If the aspartate residue is only involved in intermediate formation, the steady-state k_{cat} value ($k_{cat} = k_3k_5/k_3+k_5$ in Scheme I) would only be slightly diminished. The k_{cat} value would be predicted to be $\approx$0.03 s^{-1}, calculated using the individual k_{cat} values from the D92N and S131A mutants (Table 1). If, however, Asp-92 were also critical for intermediate hydrolysis, the k_{cat} value of the double mutant would be greatly affected because intermediate hydrolysis has been made even slower ($k_{cat} \approx k_5$). The k_{cat}/K_m values (k_1k_3/k_2+k_3) would be expected to be similar to the single D92N mutant (k_{cat}/K_m = 140 $M^{-1}\cdot s^{-1}$, pH 6) because the single S131A change did not significantly affect intermediate formation. The k_{cat}/K_m value of the double mutant was 110 $M^{-1}\cdot s^{-1}$, in agreement with the value for the D92N enzyme (Table 1). In drastic contrast, the k_{cat} value (0.0009 s^{-1}) of the double mutant is $\approx$2 orders of magnitude lower than that for either mutation alone (Table 1). Rate-

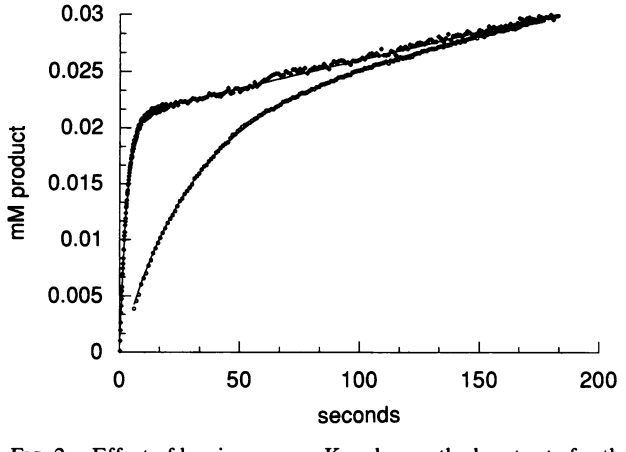

FIG. 2. Effect of leaving group pK_a value on the burst rate for the dual-specific phosphatase VHR mutant D92N/S131A. Solid diamonds represent data obtained with *p*NPP (pK_a = 7.1). Open circles represent data obtained for 4-methylumbelliferyl phosphate (pK_a = 7.8). Concentration of enzyme was 25 μM. Concentrations of *p*NPP and 4-methylumbelliferyl phosphate were 2 mM and 5 mM, respectively. Conditions were 0.1 M acetate/0.05 M Tris/0.05 M Bis-Tris, pH 7.0 at 30°C. Data were fitted as described (20).

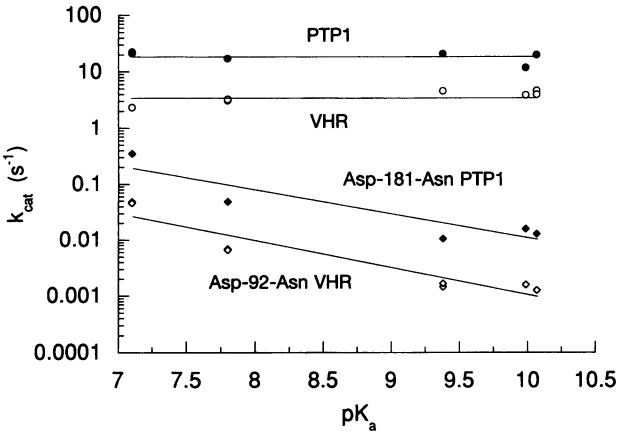

FIG. 3. Effect of leaving group pK_a value on the k_{cat} for protein-tyrosine phosphatases and dual-specific phosphatases. Filled symbols represent data with PTP1, and open symbols represent data with VHR. Circles reflect data for native enzymes. Diamonds reflect data obtained with enzymes in which the conserved general acid was changed to asparagine. Substrates *p*NPP (pK_a = 7.1), 4-methylumbelliferyl phosphate (7.8), β-naphthyl phosphate (9.38), phenyl phosphate (9.99), and phosphotyrosine (10.07) in the peptide DHTGFLTEY-VATR corresponding to mitogen-activated protein (MAP) kinase were used. Linear least-squares fitting of the Brönsted plot yielded slopes (β) of −0.5 ± 0.07 for Asp-92–Asn VHR and −0.43 ± 0.11 for Asp-181–Asn PTP1. The assay conditions were 0.1 M acetate/0.05 M Tris/0.05 M Bis-Tris, pH 7.0 at 30°C.

determining intermediate hydrolysis in the double mutant was verified by the observation of a stoichiometric burst when enzyme and *p*NPP were rapidly mixed in a stopped-flow spectrophotometer. These data strongly suggest that the conserved aspartate residue is important for intermediate hydrolysis and may act as general base, providing a 100-fold rate-enhancement.

^{31}P NMR Detection of the Phosphoenzyme Intermediate During Turnover. Using concomitant substitutions of D92N and S131A provided a means of directly observing the phosphoenzyme intermediate. The slow rate of intermediate hydrolysis relative to the rate of formation predicted that under steady-state conditions the proposed phosphoenzyme intermediate is present at stoichiometric amounts. Using ^{31}P NMR, we observed the thiol–phosphate intermediate during catalytic turnover (pH 7) (Fig. 1). The entire reaction was visualized by monitoring the distinct resonances of the thiol–phosphate intermediate (13.7 ppm), the substrate, *p*NPP (0.1 ppm), and the product, phosphate (2.4 ppm). Consistent with the steady-state and rapid-reaction kinetics, the intermediate forms quickly, before any free phosphate is detected. Between 13 and 40 min, the level of intermediate remains constant (steady-state) while the level of substrate decreases and free phosphate increases at a rate consistent with turnover (k_{cat}). Integration of the peaks revealed that >95% of the total enzyme existed as the intermediate during steady-state turnover. After complete turnover only free phosphate is detected.

Importance of General Acid Catalysis for Intermediate Formation. In addition to directly following the thiol–phosphate intermediate, the S131A substitution provided a means of monitoring intermediate formation by measuring the burst rate with rapid-reaction kinetics. Because of the large difference in rates between the two chemical steps, the faster burst rate is a measure of the rate of intermediate formation. The pH-dependence of the burst rate for the S131A enzyme mirrors the bell-shaped k_{cat}–pH profile for native VHR. With the D92N/S131A enzyme, the burst rate lacks the basic limb of the pH profile [i.e., burst rates decreased at high pH values in the S131A mutant, but did not with the D92N/S131A mutant (Table 1)]. These data are consistent with the requirement for Asp-92 being protonated for intermediate formation and suggest that chemical formation of the intermediate is the slowest step in turnover for both native VHR and the D92N mutant. Additional support for rate-limiting chemistry comes from recent ^{18}O–oxygen kinetic isotope effects experiments with the *Yersinia* PTPase and PTP1 (27). Furthermore, the rate of product burst with the D92N/S131A enzyme depended upon the leaving group pK_a of the substrate. The burst rate was 9-fold lower with 4-methylumbelliferyl phosphate (pK_a = 7.8) than with *p*NPP (pK_a = 7.1), although steady-state turnover of each was the same (Fig. 2), reflecting hydrolysis of the common thiol–phosphate intermediate.

The ease of expulsion of a leaving group depends on its pK_a value and on its state of protonation. Because both PTP1 and VHR will hydrolyze a number of substituted aryl phosphate monoesters, it was possible to explore the effect of general acid catalysis on the transition state for intermediate formation. By following the rates of hydrolysis for a series of aryl phosphate monoesters with different leaving group pK_a values, the importance of leaving group protonation on catalysis was investigated for both native and Asp → Asn mutant enzymes (Fig. 3). Asp-181 of PTP1 functions as a general acid during intermediate formation. The D181N substitution resulted in a loss of the basic limb of the bell-shaped pH profile of the k_{cat} and k_{cat}/K_m kinetic parameters (unpublished data, D.L.L., J.M.D., and J.E.D.). Loss of the basic limb was previously described for the D92N mutant of VHR. The native enzymes of VHR and PTP1 exhibited no significant dependence on leaving-group pK_a values ranging from 7 to 10. However, when the putative general acid was changed to an asparagine in both enzymes, the k_{cat} values exhibited a large dependence, indicating that expulsion of the leaving group becomes more difficult as the pK_a value is elevated. The identical trend in pK_a dependence was observed for the apparent second-order rate constant k_{cat}/K_m. Although capable of hydrogen bonding, an asparagine residue is incapable of proton donation. With the mutant enzymes, substrates with high pK_a values such as phosphotyrosine (pK_a = 10.07) are difficult to expel because the developing negative charge cannot be stabilized by proton transfer. However, substrates like *p*NPP are easier to expel because the electrons can be delocalized into the nitro substituent. General acid catalysis by the conserved aspartic acid residue is critical with the physiological substrate phosphotyrosine where proton donation can compensate for a poor leaving group. The lack of a leaving group effect observed for the native enzymes (Fig. 3) suggests that transfer of a proton to the phenolic oxygen is simultaneous with P–O bond cleavage such that no charge is developed on the phenolic oxygen. This is shown in Scheme **III**, where P–O bond breakage and transfer of the aspartic acid proton to

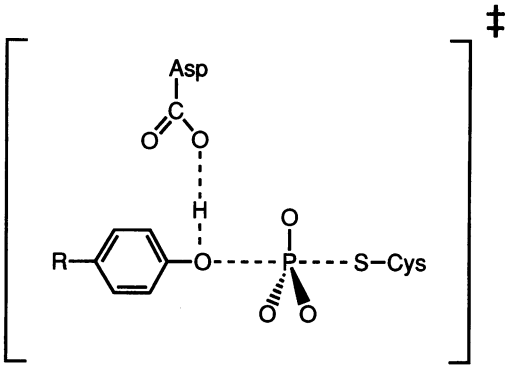

Scheme **III**

the phenolic oxygen are quite complete in the transition state.

***Yersinia* PTPase Complexed with Transition-State Analog Vanadate.** A crystal structure of the *Yersinia* PTPase complexed with vanadate has been solved to 2.2-Å resolution. The details of this work will appear elsewhere (unpublished data, J.V. and M.A.S.). Because vanadate is an unusually good inhibitor of PTPases and dual-specific phosphatases and is known to readily adopt a pentavalent geometry (28, 29), we anticipated that it could bind covalently to the active-site cysteine. Initial difference electron density maps revealed continuous electron density between the bound anion and the active-site Cys-403 nucleophile. The final refined distance between the Cys-403 Sγ and vanadium atom was 2.5 Å, consistent with a covalent bond. The structure demonstrated a distorted trigonal bipyramidal geometry that may mimic the transition state for thiol–phosphate hydrolysis (Fig. 4). Many of the key interactions revealed by this structure are in full agreement with the proposed mechanism. The close proximity of the conserved hydroxyl residue of Thr-410 in the *Yersinia* enzyme and the catalytic Cys-403 is clearly shown in Fig. 4. Moreover, the conserved Asp-356 makes a hydrogen bond of 2.8 Å to the apical oxygen of vanadate, consistent with its role as a general acid/base. The apical oxygen occupies the position where the phenolic oxygen of phosphotyrosine would be located in the Michaelis complex (16, 22) and where a water molecule would be present during the hydrolysis of the phosphoenzyme intermediate. As a general acid, the aspartic acid donates a proton to the phenolic oxygen to facilitate expulsion of tyrosine during formation of the cysteinylphosphate intermediate, and as a general base, aspartate activates a water molecule to facilitate intermediate hydrolysis. Negative charge on equatorial oxygens of the phosphate is stabilized by a bidentate interaction with the conserved arginine and by the backbone amide N-H groups of the conserved active-site loop (15, 16, 22, 30).

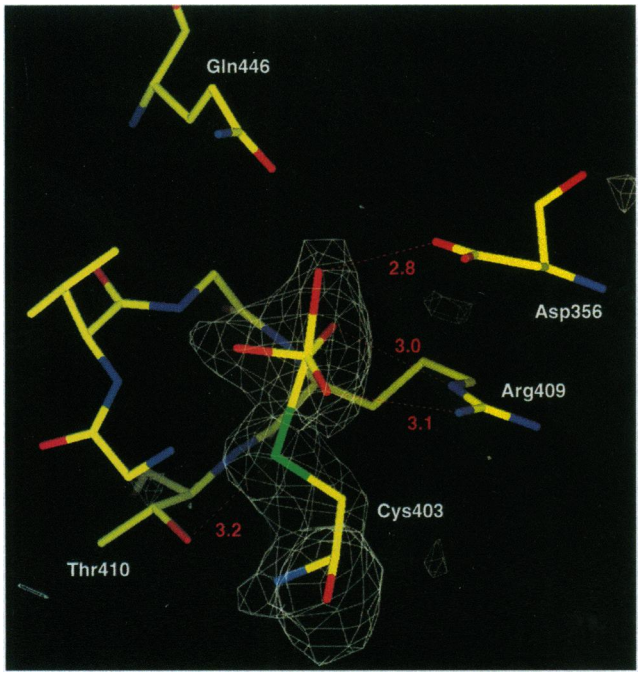

FIG. 4. Vanadate covalently bound to the active-site Cys-403 of the *Yersinia* PTPase mimics the catalytic transition state. The *Yersinia* PTPase was cocrystallized with 1 mM sodium vanadate at pH 8.0, and the structure was solved by molecular replacement. The difference electron density shown (contoured at 3.0σ) was calculated from the refined coordinates after omitting contribution of both Cys-403 and the vanadate from the calculated structure factors. Important distances are drawn in red, including the conserved general acid/base Asp-356 and the hydroxyl residue of Thr-410.

In summary, our data support the concept that the PTPases and dual-specific phosphatases use a common catalytic strategy. The mechanism employs a thiol–phosphate enzyme intermediate and two transition states. Under most conditions the rate-limiting step in the reaction appears to be formation of the phosphoenzyme intermediate. Substitution of a critical Ser/Thr residue in the active-site sequence HCXXGXXRS(T) leads to a dramatic change in the rate-limiting step in the reaction, such that intermediate hydrolysis becomes rate-limiting. By using amino acid substitutions that isolate the two chemical steps, general acid catalysis during intermediate formation and general base catalysis during intermediate hydrolysis by the same aspartate residue were demonstrated. This approach has allowed us to directly visualize the phosphoenzyme intermediate during catalysis. Additional support for the proposed mechanism has been obtained by x-ray structural analysis of a transition-state analog covalently bound to a PTPase.

We thank Dr. Scott Woehler for assistance with the NMR and Michelle Shukait for assistance in the preparation of the manuscript. This research was supported by National Institutes of Health (NIH) Grants NIDDKD 18024, 18849 (J.E.D.), and R01 AI34095 (M.A.S.) and The University of Michigan Multipurpose Arthritis Center (NIH Grant P560 AR20557). J.M.D. is the recipient of an Individual National Research Service award (1F32GM17789-01). M.A.S. is a Pew Scholar in the Biomedical Sciences.

1. Koretzky, G. A., Picus, J., Schultz, T. & Weiss, A. (1991) *Proc. Natl. Acad. Sci. USA* **88,** 2037–2041.
2. Pani, G., Kozlowski, M., Cambier, J. C., Mills, G. B. & Siminovitch, K. A. (1995) *J. Exp. Med.* **181,** 2077–2084.
3. Sato, T., Irie, S., Kitada, S. & Reed, J. C. (1995) *Science* **268,** 411–415.
4. Guan, K. L. & Dixon, J. E. (1990) *Science* **249,** 553–556.
5. Bliska, J. B., Guan, K. L., Dixon, J. E. & Falkow, S. (1991) *Proc. Natl. Acad. Sci. USA* **88,** 1187–1191.
6. Guan, K. L., Broyles, S. S. & Dixon, J. E. (1991) *Nature (London)* **350,** 359–362.
7. Ishibashi, T., Bottaro, D. P., Chan, A., Miki, T. & Aaronson, S. A. (1992) *Proc. Natl. Acad. Sci. USA* **89,** 12170–12174.
8. Russell, P. & Nurse, P. (1986) *Cell* **45,** 145–153.
9. Gautier, J., Solomon, M. J., Booher, R. N., Bazan, J. F. & Kirschner, M. W. (1991) *Cell* **67,** 197–211.
10. Sun, H., Charles, C. H., Lau, L. F. & Tonks, N. K. (1993) *Cell* **75,** 487–493.
11. Ward, Y., Gupta, S., Jensen, P., Wartmann, M., Davis, R. J. & Kelly, K. (1994) *Nature (London)* **367,** 651–654.
12. Guan, K. L. & Dixon, J. E. (1991) *J. Biol. Chem.* **266,** 17026–17030.
13. Cho, H., Krishnaraj, R., Kitas, E., Bannwarth, W., Walsh, C. T. & Anderson, K. S. (1992) *J. Am. Chem. Soc.* **114,** 7296–7298.
14. Zhou, G., Denu, J. M., Wu, L. & Dixon, J. E. (1994) *J. Biol. Chem.* **269,** 28084–28090.
15. Barford, D., Flint, A. J. & Tonks, N. K. (1994) *Science* **263,** 1397–1404.
16. Stuckey, J. E., Schubert, H. L., Fauman, E. B., Zhang, Z.-Y., Dixon, J. E. & Saper, M. A. (1994) *Nature (London)* **370,** 571–575.
17. Denu, J. M., Zhou, G., Guo, Y. & Dixon, J. E. (1995) *Biochemistry* **34,** 3396–3403.
18. Zhang, Z.-Y. & Dixon, J. E. (1994) *Proc. Natl. Acad. Sci. USA* **91,** 1624–1627.
19. Denu, J. M., Zhou, G., Wu, L., Zhoa, R., Yuvaniyama, J., Saper, M. A. & Dixon, J. E. (1995) *J. Biol. Chem.* **270,** 28084–28090.
20. Denu, J. M. & Dixon, J. E. (1995) *Proc. Natl. Acad. Sci. USA* **92,** 5910–5914.
21. Zhang, Z.-Y. & Van Etten, R. L. (1991) *J. Biol. Chem.* **266,** 1516–1525.
22. Jia, Z., Barford, D., Flint, A. J. & Tonks, N. K. (1995) *Science* **268,** 1754–1758.
23. Gregoret, L. M., Rader, S. D., Fletterick, R. J. & Cohen, F. E. (1991) *Proteins* **9,** 99–107.
24. Fersht, A. R. (1987) *Trends Biochem. Sci.* **12,** 301–304.

25. Sieck, L. W. & Meot-Ner, M. (1989) *J. Phys. Chem.* **93,** 1586–1588.
26. Jeng, M.-F., Holgren, A. & Dyson, H. J. (1995) *Biochemistry* **34,** 10101–10105.
27. Hengge, A. C., Sowa, G., Wu, L. & Zhang, Z.-Y. (1995) *Biochemistry* **34,** 13982–13987.
28. VanEtten, R. L., Waymack, P. P. & Rehkop, D. M. (1974) *J. Am. Chem. Soc.* **96,** 6782–6785.
29. Wlodawer, A., Miller, M. & Sjolin, L. (1983) *Proc. Natl. Acad. Sci. USA* **80,** 3628–3631.
30. Zhang, Z.-Y., Wang, Y., Wu, L., Fauman, E., Stuckey, J., Schubert, H., Saper, M. A. & Dixon, J. E. (1995) *Biochemistry* **33,** 15266–15270.